



# Low-temperature direct copper-to-copper bonding enabled by creep on highly (111)-oriented Cu surfaces

Chien-Min Liu,<sup>a</sup> Han-wen Lin,<sup>a</sup> Yi-Cheng Chu,<sup>a</sup> Chih Chen,<sup>a,\*</sup> Dian-Rong Lyu,<sup>b</sup>  
Kuan-Neng Chen<sup>b</sup> and K.N. Tu<sup>c</sup>

<sup>a</sup>Department of Materials Science and Engineering, National Chiao Tung University, Hsinchu, Taiwan 30010, Republic of China

<sup>b</sup>Department of Electronics Engineering, National Chiao Tung University, Hsinchu, Taiwan 30010, Republic of China

<sup>c</sup>Department of Materials Science and Engineering, University of California at Los Angeles, Los Angeles, CA 90095, USA

Received 11 January 2014; accepted 31 January 2014

Available online 7 February 2014

We achieve low-temperature Cu-to-Cu direct bonding using highly (111)-oriented Cu films. The bonding temperature can be lowered to 200 °C at a stress of 114 psi for 30 min at  $10^{-3}$  torr. The temperature is lower than the reflow temperature of 250 °C for Pb-free solders. Our breakthrough is based on the finding that the Cu (111) surface diffusivity is the fastest among all the planes of Cu and the bonding process can occur through surface diffusion creep on the (111) surfaces.

© 2014 Acta Materialia Inc. Published by Elsevier Ltd. All rights reserved.

**Keywords:** Cu-to-Cu direct bonding; Creep; Diffusion; Preferred orientation

Solders have been widely adopted as interconnect materials for microelectronic devices since 1969 [1], because solders have low melting points and solder joint technology is very forgiving [2–4]. The melting point for the eutectic SnPb solder is 183 °C and the reflow temperature is approximately 200 °C. As environment concerns draw increasing attention, Pb-free solders have replaced Pb-containing solders for interconnects. The most popular Pb-free solders are Sn-rich, including such species as SnAg and SnAgCu, and their melting points are over 230 °C [5]. The reflow temperature is approximately 250 °C. In addition, the metallurgical reaction rates between Pb-free solders and Cu/Ni metallization are faster than those between Pb-containing solders and Cu/Ni metallization, resulting in extensive formation of intermetallic compounds (IMC) [5].

In addition, as the scaling of large-scale integrated circuits (ICs) approaches the physical limit, three dimensional (3-D) ICs have emerged as the most promising solution [6–8]. Silicon chips are stacked vertically to shorten the wiring between chips, and through-silicon-vias and microbumps are adopted for

interconnects between chips. The thickness of the solder decreases to about 5–10 μm in microbumps [6–12]. However, the volume fraction of IMCs in a microbump increases significantly. The Cu–Sn and Ni–Sn IMCs are brittle in nature [13,14]. The brittleness of the microbumps will become a yield and reliability issue. Furthermore, necking of solder may occur in microbumps during reflow and solder-state aging [15]. Therefore, many new reliability issues arise in solder-based microbumps for 3-D IC.

An alternative approach for the vertical interconnects is to eliminate solder by using Cu-to-Cu direct bonding. Such Cu-to-Cu microbumps have better electrical and thermal conductivity properties than solder microbumps. Many studies have been carried out on Cu-to-Cu direct bonding. Such bonding can be realized in an ultrahigh vacuum at room temperature, provided that the surfaces of the two Cu components are atomically flat, and the surfaces must be activated by a special cleaning process [16]. Thus, this approach is time consuming and expensive. Cu direct bonding can also be accomplished by thermal compression bonding at 300 °C in an ordinary vacuum of  $10^{-3}$  torr [17–19]. However, the high bonding temperature limits the types of possible applications.

In this study, we report a simple process to achieve the Cu-to-Cu direct bonding at 200 °C for 30 min under

\* Corresponding author. Tel.: +886 3 5731814; fax: +886 3 5724727; e-mail: [chih@mail.nctu.edu.tw](mailto:chih@mail.nctu.edu.tw)

114 psi (0.78 MPa) of compression in ordinary vacuum conditions. At least one of the Cu films used in direct bonding must possess a highly (111)-oriented surface, because this has the fastest surface diffusivity of all the crystallographic planes [20–22]. Cross-sectional transmission electron microscopy (TEM) was used to examine the bonding interfaces (grain boundaries), and the results indicate that oxide-free and almost void-free grain boundaries have been obtained through this approach.

We prepared two types of Cu films for Cu–Cu direct bonding: highly (111)-oriented Cu films and randomly oriented Cu films. To fabricate the (111)-oriented Cu film, a 100 nm thick Ti adhesion layer and a 200 nm thick Cu film were sequentially sputtered on a 20 cm Si wafer using an Oerlikon Cluster Line 300. To bond the Cu films, the samples were cut into  $3 \times 3 \text{ mm}^2$  pieces. Randomly oriented Cu films were prepared by sputtering using Ion Tech Microvac 450CB. Then, the pieces were cleaned ultrasonically in acetone for 5 min, dried with an  $\text{N}_2$  purge, cleaned with a mixed solution of HCl and deionized water (DI) at a ratio of 1:1 for 30 s, rinsed with DI water and purged with  $\text{N}_2$  gas again. Next, the Cu films were placed face to face and fastened using a screw clamp. The bonding pressure was measured to be 114 psi (0.78 MPa) using a mechanical gauge at room temperature. The specimens were loaded into a quartz furnace tube, to which a vacuum was applied using a mechanical pump. The pressure was approximately  $1 \times 10^{-3}$  torr. The furnace was heated to 200 °C at a ramping rate of  $1.3 \text{ °C s}^{-1}$ , and all cooling events were achieved by allowing the furnace to cool naturally. The bonding conditions were 200 °C for 10 min, 30 min and 1 h. The microstructures for the bonded Cu–Cu interfaces were examined with a JEOL-2100 scanning transmission electron microscope. The TEM examinations were performed at 200 kV, with a point-to-point resolution of 0.23 nm and a lattice resolution of 0.14 nm. Analysis using an energy-dispersive X-ray spectrometer (EDS) was performed on a Link ISIS 300 EDS attached to the JEOL-2100 microscope and was used to determine the compositional distribution of oxidation within the local areas of the samples in the Cu-bonded layers. X-ray diffraction (XRD) and electron backscatter diffraction (EBSD) were used to analyze the orientation and grain orientations of the Cu films. The EBSD measurements were performed using a JEOL 7001F field emission scanning electron microscope with an EDAX/TSL system operated at 25 kV. OIM™ software was used to analyze the orientation maps and crystallographic textures based on Kikuchi patterns.

Almost void-free bonding can be achieved at 200 °C between the two highly (111)-oriented Cu films. Figure 1(a) presents a bright-field cross-sectional TEM image for two highly (111)-oriented Cu films bonded at 200 °C for 1 h. Virtually no voids can be seen at the bonding interface. Figure 1(b) shows the corresponding dark-field TEM image using the  $(11\bar{1})$  diffraction. The selected area diffraction pattern is shown in the bottom-right corner, and has a  $[011]$  pole. The results indicate that the columnar Cu grains in both films are  $\langle 111 \rangle$ -oriented. Figure 1(c) is a high-resolution TEM

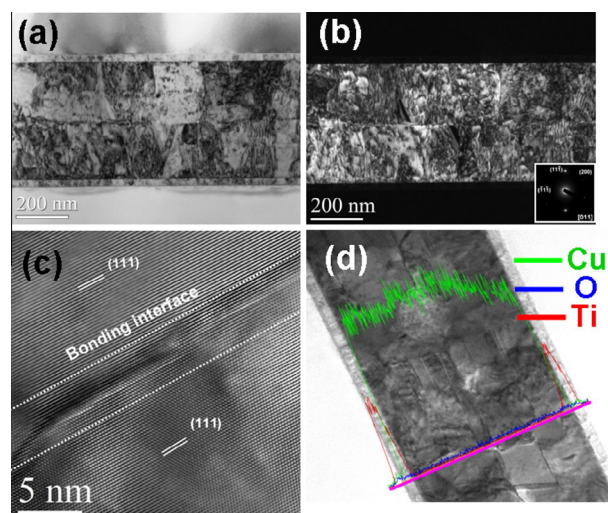


**Figure 1.** (a) Bright-field TEM image of two highly (111)-oriented films bonded at 200 °C for 1 h. (b) Corresponding dark-field TEM image using  $(11\bar{1})$  diffraction. The selected area diffraction (SAD) pattern is shown in the bottom-right corner. (c) Cross-sectional high-resolution TEM image of the bonding interface after annealing 200 °C for 1 h. (d) TEM EDS line-scan across the entire sample in (a).

image of the bonding interface. No amorphous layer was found and the lattice points were continuous across the bonding interface. Figure 1(d) depicts an EDS line scan across the bonded sample. No obvious oxygen signals were detected at the interface. These results reveal the formation of excellent bonding interfaces or grain boundaries.

Such strong bonding interfaces could also be accomplished when the bonding time was shortened to 30 min. Figure 2(a) presents a cross-sectional bright-field TEM image for the (111)-oriented Cu films bonded at 200 °C for 30 min. Virtually no voids can be seen at the smooth bonding interface. However, many voids may exist at the bonding interface when the bonding time is further decreased to 10 min. Figure 2(b) shows the bonded (111)-oriented Cu films at 200 °C for 10 min, with many voids remaining in the interface after the 10 min annealing. The above results indicate that

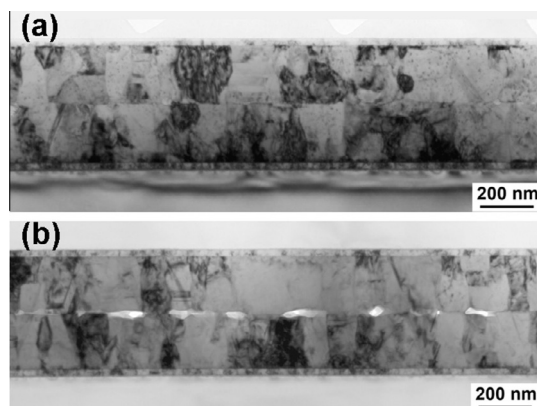


**Figure 2.** (a) Bright-field TEM image of two highly (111)-oriented films bonded at 200 °C for 30 min. (b) Bright-field TEM image of two highly (111)-oriented films bonded at 200 °C for 10 min.

annealing at 200 °C for 30 min can provide excellent bonding between two strongly (111)-oriented Cu films. Tensile tests were performed on  $2 \times 2$  cm specimens bonded at 200 °C for 1 h, and the bonded interface possesses high strength values. Three of the specimens that exhibited excellent bonding quality survived tensile testing in excess of 175 kg. Therefore, the bonding interfaces have excellent bonding strength [24,25].

The above approach provides a breakthrough in Cu-to-Cu direct bonding. The bonding temperature can be lowered to 200 °C, which is lower than that required when using solders. The critical reason for the breakthrough is the fast diffusion of Cu atoms on the Cu (111) surfaces. The bonding process was triggered and achieved by Nabarro–Herring (or Coble) creep [23], because the two Si chips and Cu films were under compressive stress and at an elevated temperature. At the initial stage of bonding, the Cu at the contact regions was under a high compressive stress, whereas the Cu away from the contact regions (cavities) is subjected to less or no compressive stress. As there is a stress gradient, the Cu atoms in the high compressive region diffuse to the cavity region, thereby eliminating the cavity (void) and forming a bond. The calculated theoretical diffusivities are  $9.42 \times 10^{-6}$ ,  $1.19 \times 10^{-9}$  and  $5.98 \times 10^{-11}$   $\text{cm}^2 \text{s}^{-1}$  for the (111), (100) and (110) planes, respectively. Therefore, the much faster surface diffusion on the (111)-oriented grains will facilitate the Cu-to-Cu direct bonding. The majority of grains in the above samples were (111)-oriented.

Figure 3(a) presents a plan-view EBSD orientation image map, and the inverse pole figure is illustrated in the bottom-right corner. The results indicate that 97% of the surface grains are (111)-oriented and the grain size is 195 nm on average. XRD also supports the EBSD results. Figure 3(d) shows the XRD, and the count for the (111) plane appears to be very high, though the (200) peak is invisible in the pattern. Therefore, the Cu film has a very strongly preferred (111) orientation.

Bonding can also be achieved between a (111)-oriented Cu film and a randomly oriented Cu film. Figure 4(a) presents a plan-view TEM image for the randomly oriented Cu film, with the selected area diffraction pattern shown in the bottom-left corner. The result indicates that the randomly oriented Cu film is polycrystalline. Figure 4(b) illustrates the XRD, in which the Cu (200) is visible. The results indicate that the grains are randomly oriented. Figure 4(c) presents a cross-sectional bright-field TEM image for a randomly oriented Cu film (top) bonded to a highly (111)-oriented Cu film (bottom) at 200 °C for 30 min. The bonding interface is good, but with more voids than in the image shown in Figure 1. This may be attributed to the fact that only one of the Cu films is (111)-oriented.

Figure 4(d) shows the corresponding dark-field TEM image using (111) diffraction. The grains on the top film are invisible because they are not (111)-oriented. The Cu grains on the randomly oriented Cu film grew and consumed some of the (111)-oriented Cu grains. Because the initial grain size on the randomly oriented Cu film is about 20 nm, there are many grain boundaries. Grain growth may occur inside the film first, thus many large grains were observed in the film after the

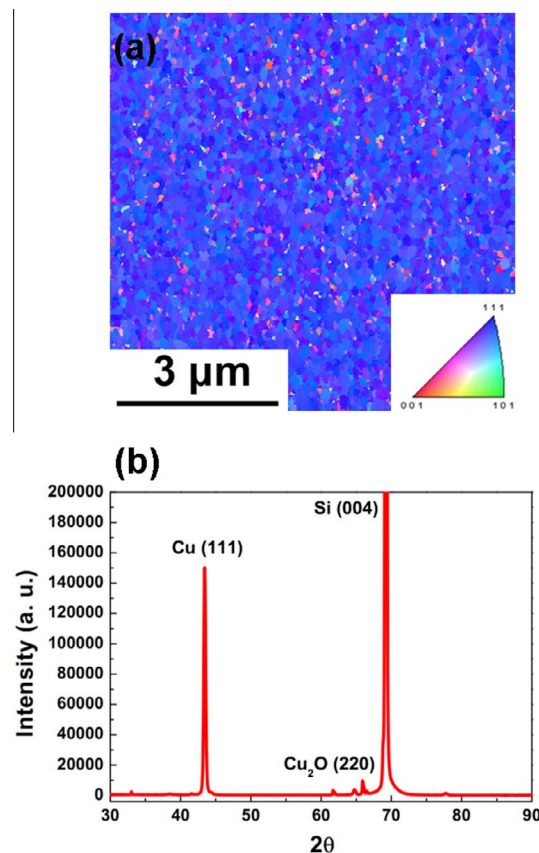


Figure 3. (a) Plan-view EBSD orientation image map of the highly (111)-oriented film. (b) XRD pattern of the highly (111)-oriented film.

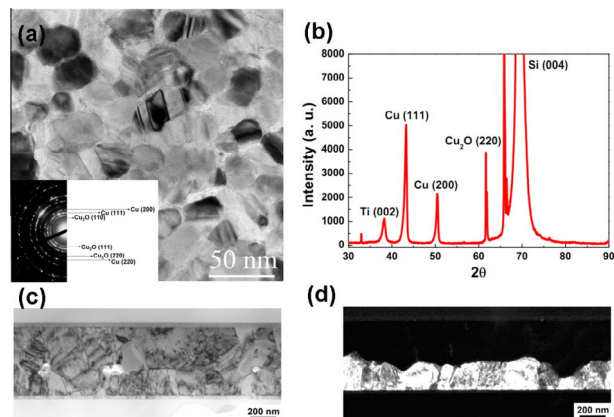


Figure 4. (a) Plan-view TEM image map of the randomly oriented Cu film. The SAD pattern is shown in the bottom-left corner. (b) XRD pattern for the randomly oriented Cu film. (c) Bright-field TEM image of a highly (111)-oriented film bonded to a randomly oriented Cu film on the top at 200 °C for 30 min. (d) Corresponding dark-field TEM image for the sample in (a) using (111) diffraction of the highly (111)-oriented film.

bonding. In addition, the bonding interface moved toward to the (111)-oriented film, which may be attributed to a ripening effect.

In summary, we have achieved low-temperature bonding using highly (111)-oriented Cu films. With the aid of fast Cu diffusion on (111) planes, the bonding conditions can be lowered to 200 °C for 30 min under

114 psi in an ordinary vacuum. An almost void-free and oxide-free interface can be achieved by bonding two highly (111)-oriented Cu films. In addition, an excellent interface with few voids can also be achieved between a highly (111)-oriented Cu film and a randomly oriented Cu film. This approach offers a huge improvement over the interconnect materials currently used in 3-D IC.

Financial support from the National Science Council, Taiwan, under contract NSC 99-2221-E-009-040-MY3, is acknowledged. The authors thank the Center for Micro/Nano Science and Technology (CMNST) at National Cheng Kung University for assistance with the analytical equipment.

- [1] L.F. Miller, *IBM J. Res. Dev.* 13 (3) (1969) 239.
- [2] K.N. Tu, *Solder Joint Technology*, Springer, New York, 2007.
- [3] N. Chawla, *Int. Mater. Rev.* 54 (2009) 368.
- [4] C.K. Chung, J.G. Duh, C.R. Kao, *Scr. Mater.* 63 (2010) 258.
- [5] K. Zeng, K.N. Tu, *Mater. Sci. Eng. R* 38 (2002) 55.
- [6] R.S. Patti, *Proc. IEEE* 94 (2006) 1214.
- [7] M.T. Fukushima, T. Tanaka, *Proc. IEEE* 97 (2009) 49.
- [8] J.-Q. Lu, *Proc. IEEE* 97 (2009) 18.
- [9] H.Y. Hsiao, C.M. Liu, H.W. Lin, T.C. Liu, C.L. Lu, Y.S. Huang, C. Chen, K.N. Tu, *Science* 336 (2012) 1007.
- [10] K.N. Tu, *Microelectron. Reliab.* 51 (2011) 517.
- [11] T.C. Liu, C.M. Liu, Y.S. Huang, C. Chen, K.N. Tu, *Scr. Mater.* 68 (2013) 241.
- [12] Y.S. Huang, H.Y. Hsiao, C. Chen, K.N. Tu, *Scr. Mater.* 66 (2012) 741.
- [13] K.E. Yazzie, H.X. Xie, J.J. Williams, N. Chawla, *Scr. Mater.* 66 (2012) 586.
- [14] K.E. Yazzie, H.E. Fei, H. Jiang, N. Chawla, *Acta Mater.* 60 (2012) 4336.
- [15] Y.C. Liang, H.W. Lin, H.P. Chen, C. Chen, K.N. Tu, Y.S. Lai, *Scripta Mater.* 69 (2013) 25.
- [16] T.H. Kim, M.M.R. Howlader, T. Itoh, T. Suga, *J. Vac. Sci. Technol. A* 21 (2003) 449.
- [17] C.S. Tan, L. Peng, J. Fan, H. Li, S. Gao, *IEEE Trans. Device Mater. Reliab.* 12 (2012) 194.
- [18] J. Lee, D.M. Fernandez, M. Paing, Y.C. Yeo, S. Gao, *IEEE Trans. Comp. Packag. Manuf. Technol.* 2 (2012) 964.
- [19] K. N. Chen, S. H. Lee, Paul S. Andry, Cornelia K. Tsang, Anna W. Topol, Y. M. Lin, J. Q. Lu, Albert M. Young, M. Jeong, W. Haensch, 2006 International Electron Devices Meeting (IEDM), San Francisco CA, December 11–13, 2006.
- [20] P.M. Agrawal, B.M. Rice, D.L. Thompson, *Surf. Sci.* 515 (2003) 21.
- [21] D.B. Butrymowicz, J.R. Manning, M.E. Read, *J. Phys. Chem. Ref. Data* 2 (1973) 643.
- [22] C.N. Liao, Y.C. Lu, D. Xu, *J. Electrochem. Soc.* 160 (2013) D207.
- [23] F.A. Mohamed, K.L. Murty, J.W. Jr, Morris, *Metall. Trans.* 4 (1973) 935.
- [24] K.N. Chen, S.M. Chang, L.C. Shen, R. Reif, *J. Electron. Mater.* 35 (2006) 1082.
- [25] K. N. Chen, T. M. Shaw, C. Cabral, Jr., G. Zuo, 2010 International Electron Devices Meeting (IEDM), San Francisco CA, December 6–8, 2010.